Templating Route to Mesoporous Nanocrystalline Titania Nanofibers

Weon-Sik Chae, Sang-Wook Lee, and Yong-Rok Kim*

Photon Applied Functional Molecule Research Laboratory, Department of Chemistry, Yonsei University, Seoul 120-749, South Korea

Received March 18, 2005
Revised Manuscript Received May 6, 2005

Currently, titania (TiO_2)-based solid composites have attracted much attention as advanced materials due to their unique properties, such as catalytic, electronic, photoconducting, and molecular sensing properties.[1] In particular, since a mesoporous system typically provides a tunable pore size and high specific surface area,[2] mesoporous titania (MPT) has the additional advantages of molecular sieving effect, high reactivity, and enhanced sensing ability. To date, the MPT materials have been typically fabricated in bulk powder and film.[3] For the specialized purposes of energy conversion and molecular sensor devices, one-dimensional (1D) morphology of MPT has distinctive advantages. Despite such merits, few studies have tried to fabricate 1D MPT nanomaterial[4] because of the high reactivity of hydrolysis and condensation of titania precursor.[5] Therefore, a careful synthetic strategy is required to fabricate 1D crystalline titania mesoporous material, which is still a challenging work.

In this study, we have newly fabricated 1D MPT nanofibers by using porous alumina as a morphology-directing "hard template". Within the cylindrical nanochannels of porous alumina, an amphiphilic triblock copolymer (Pluronic F127; $EO_{106}PO_{70}EO_{106}$) was used as a structure-directing "soft template" to make the mesoporous structure. For the titania introduction within the "soft template", titanium(IV) isopropoxide was added in an acidic ethanol solution containing the Pluronic F127. To fabricate MPT nanomaterials with different pore sizes, a different amount (2.84 and

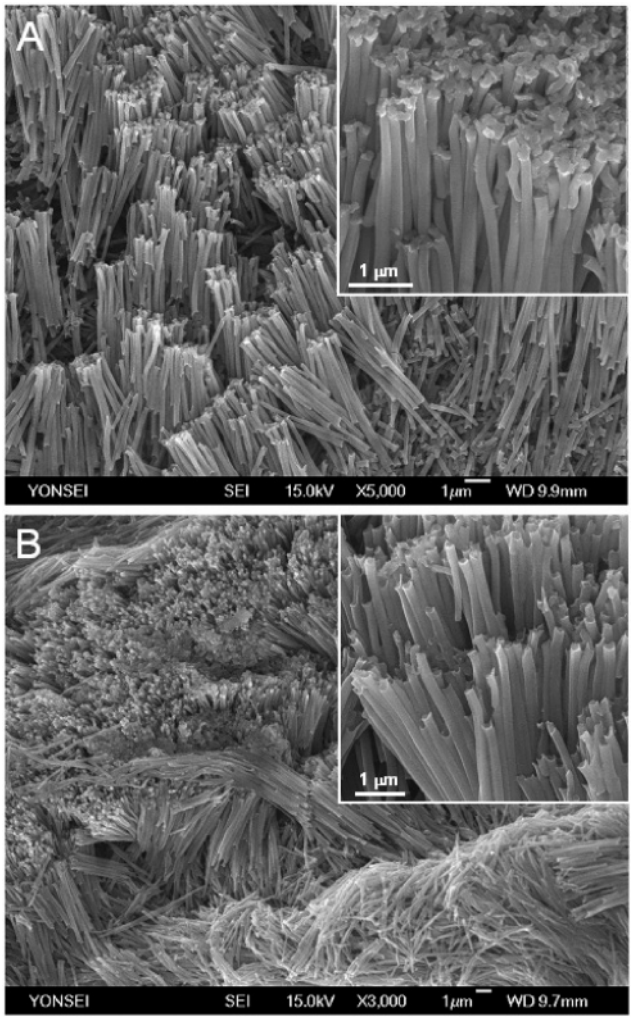

Figure 1. FE-SEM images of the mesoporous titania nanofibers: (A) MPT-1 and (B) MPT-2. The insets are the magnified images of the corresponding nanofibers.

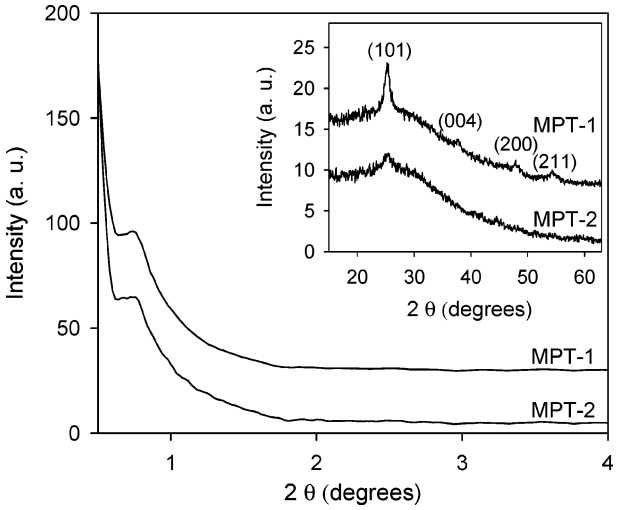

Figure 2. X-ray diffraction patterns of the mesoporous titania nanofibers in a small-angle region. The inset is the diffraction patterns of the mesoporous titania nanofibers in a wide-angle region.

* To whom correspondence should be addressed. Telephone: +82 (0)2 2123 2646. Fax: +82 (0)2 364 7050. E-mail: yrkim@yonsei.ac.kr.

(1) (a) Hagfeldt, A.; Grätzel, M. *Chem. Rev.* **1995**, *95*, 49. (b) Mora-Seró, I.; Bisquert, J. *Nano Lett.* **2003**, *3*, 945. (c) Bartl, M. H.; Puls, S. P.; Tang, J.; Lichtenegger, H. C.; Stucky, G. D. *Angew. Chem., Int. Ed.* **2004**, *43*, 3037. (d) Sakai, N.; Ebina, Y.; Takada, K.; Sasaki, T. *J. Am. Chem. Soc.* **2004**, *126*, 5851. (e) Topoglidis, E.; Campbell, C. J.; Cass, A. E. G.; Durrant, J. R. *Langmuir* **2001**, *17*, 7899.

(2) (a) Zhao, D.; Huo, Q.; Feng, J.; Chmelka, B. F.; Stucky, G. D. *J. Am. Chem. Soc.* **1998**, *120*, 6024. (b) Kruk, M.; Jaroniec, M.; Sakamoto, Y.; Terasaki, O.; Ryoo, R.; Ko, C. H. *J. Phys. Chem. B* **2000**, *104*, 292. (c) Li, D.; Zhou, H.; Honma, I. *Nat. Mater.* **2004**, *3*, 65. (d) Marlow, F.; Spliethoff, B.; Tesche, B.; Zhao, D. *Adv. Mater.* **2000**, *12*, 961. (e) Marlow, F.; Kleitz, F. *Microporous Mesoporous Mater.* **2001**, *44*−*45*, 671. (f) Wang, J.; Zhang, J.; Asoo, B. Y.; Stucky, G. D. *J. Am. Chem. Soc.* **2003**, *125*, 13966. (g) Wang, J.; Tsung, C.-K.; Hong, W.; Wu, Y.; Tang, J.; Stucky, G. D. *Chem. Mater.* **2004**, *16*, 5169.

(3) (a) Alberius, P. C. A.; Frindell, K. L.; Hayward, R. C.; Kramer, E. J.; Stucky, G. D.; Chmelka, B. F. *Chem. Mater.* **2002**, *14*, 3284. (b) Bosc, F.; Ayral, A.; Albouy, P.-A.; Datas, L.; Guizard, C. *Chem. Mater.* **2004**, *16*, 2208. (c) Yang, P.; Zhao, D.; Margolese, D. I.; Chmelka, B. F.; Stucky, G. D. *Chem. Mater.* **1999**, *11*, 2813.

(4) Madhugiri, S.; Sun, B.; Smirniotis, P. G.; Ferraris, J. P.; Balkus Jr., K. J. *Microporous Mesoporous Mater.* **2004**, *69*, 77.

(5) (a) Soler-Illia, G. J. A. A.; Sanchez, C.; Lebeau, B.; Patarin, J. *Chem. Rev.* **2002**, *102*, 4093. (b) Choi, S. Y.; Mamak, M.; Coombs, N.; Chopra, N.; Ozin, G. A. *Adv. Funct. Mater.* **2004**, *14*, 335.

10.1021/cm050603f CCC: $30.25 © 2005 American Chemical Society
Published on Web 05/20/2005

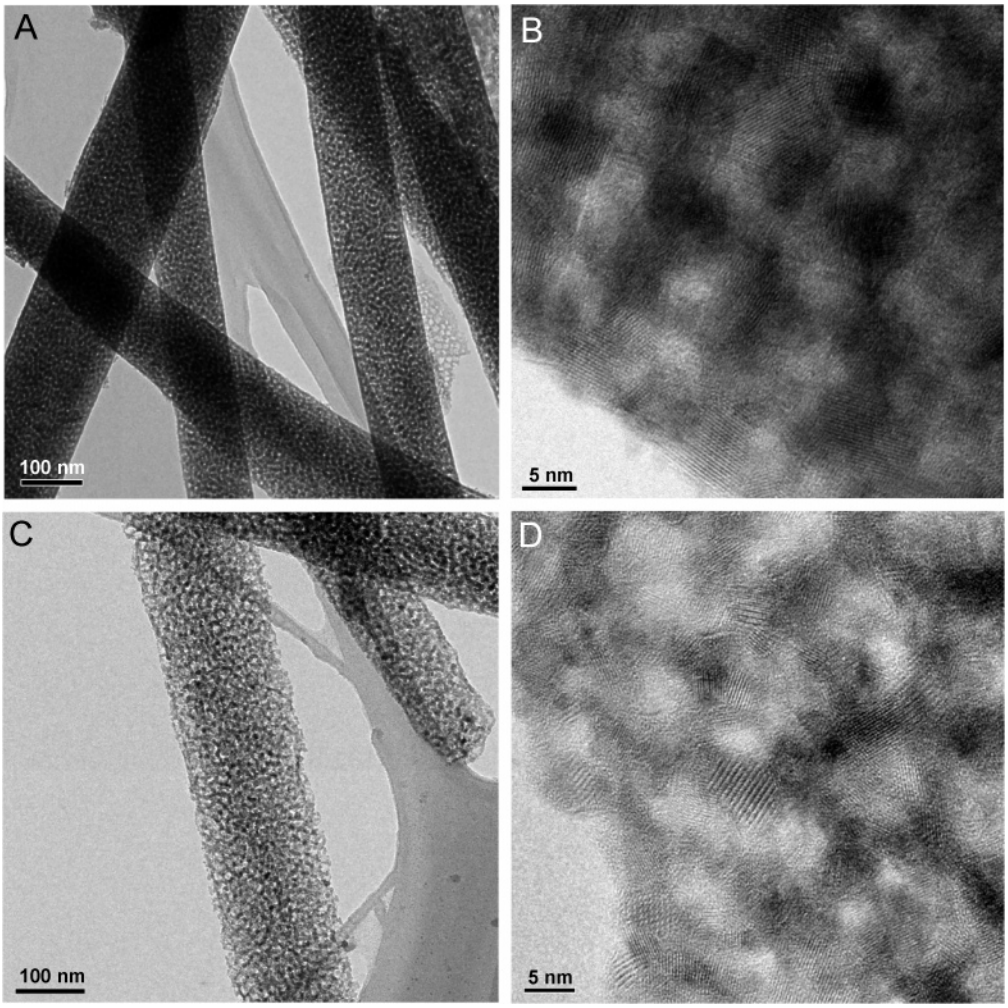

Figure 3. TEM images of the mesoporous titania nanofibers: (A) MPT-1 and (C) MPT-2. HR-TEM images are also presented for (B) MPT-1 and (D) MPT-2.

1.64 g) of titanium(IV) isopropoxide was used for preparation of the sol mixtures. Subsequently, these sol mixtures were infiltrated within the porous alumina "hard template", and they became a gel within the template. After consecutive removal of the triblock copolymer "soft template" and the porous alumina "hard template" by calcination and dissolution, respectively, 1D MPT nanofibers could be easily obtained (see Supporting Information for experimental details). The resulting nanofiber materials are denoted hereafter as MPT-1 and MPT-2 depending on the different amounts (2.84 and 1.64 g) of titanium(IV) isopropoxide used in the reaction, respectively.

Figure 1 shows the field emission scanning electron microscope (FE-SEM) images of the resulting titania nanomaterials. The MPT-1 nanomaterial, which is fabricated by using the porous alumina "hard template" with a channel diameter of 200 ± 20 nm, is shown to have a fiber shape (Figure 1A). The typical diameter and length of the fiber are estimated to be 170−210 nm and 5−9 μm, respectively. The diameter of the MPT-1 nanofiber is comparable to the channel diameter of the porous alumina template. The MPT-2 nanomaterial also exhibits a nanofiber morphology (Figure 1B) of which the diameter and length (170−210 nm and 5−8 μm) are shown to be similar to those of MPT-1.

Figure 2 shows the X-ray diffraction patterns for the MPT nanofibers in small-angle and wide-angle regions. In the small-angle diffraction region, both nanofibers present only one broad diffraction positioned at around 0.75° in 2θ (d-spacing = ∼11.7 nm). This d-spacing is similar to the reported values of the mesoporous materials that are fabricated by using Pluronic F127 template.[6] After the diffraction peak position, a simple exponential-decay-like curve is observed in the small-angle region of 0.9−4° without any

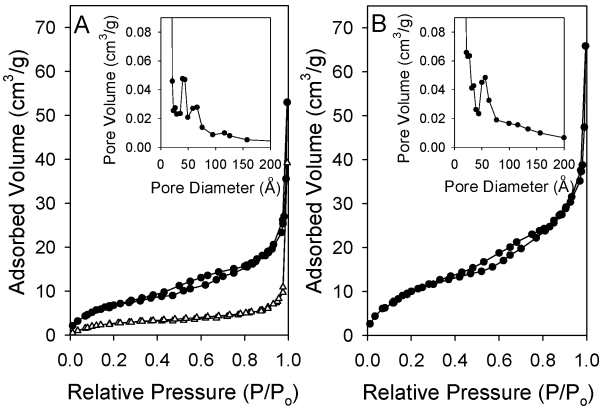

Figure 4. Nitrogen gas adsorption−desorption isotherms of the mesoporous titania nanofibers of (A) MPT-1 and (B) MPT-2 that are confined within porous alumina. Nitrogen adsorption−desorption isotherm for the empty porous alumina is also presented (triangle). The insets are pore size distribution estimated by applying a Barrett−Joyner−Halenda (BJH) method to the adsorption branches of the corresponding nanofibers.

discernible diffraction peaks, which implies a lack of mesostructural ordering for both MPT nanofibers. In the wide-angle diffraction region (inset of Figure 2), however, several diffraction peaks are observed on the MPT-1 nanomaterial. Since these peaks are well-matched with the diffraction patterns of anatase titania (JCPDS card No. 21-1272), it can be suggested that the titania building blocks constructing the MPT-1 nanofiber have anatase crystalline phase. From the diffraction peak broadening that is typically observed with decreasing crystal size,[7] the average crystal size of the titania building blocks is estimated to be ~6.5 nm based on a diffraction peak from the (101) plane. For the MPT-2 nanofiber, only one distinguishable peak is observed at the diffraction position corresponding to the (101) plane, which is possibly due to a thinner wall framework compared with that of MPT-1 as discussed below.

Transmission electron microscope (TEM) images reveal that the MPT nanofibers have a mesoporous structure with a wormlike nanochannel network inside of the nanofibers and the wall frameworks consist of nanocrystalline titania with a crystal size of 3−8 nm (Figure 3). These nanocrystalline phases of the titania building blocks constructing the wall framework are shown to be in random orientation. When a reduced amount of titanium(IV) isopropoxide is used for fabrication, i.e., from 2.84 to 1.64 g, the thickness of the wall framework becomes thinner. The high-resolution TEM (HR-TEM) images indicate that the wall thicknesses are 5−8 nm for MPT-1 and 3−5 nm for MPT-2. Since the *d*-spacing, which is a summation of the wall thickness and pore diameter, is similarly observed for both nanofibers, it is generally expected that pore diameter inversely increases with reducing wall thickness.

Figure 4 shows nitrogen gas adsorption−desorption isotherms for the MPT nanofibers confined within porous alumina as well as the empty porous alumina. Although only MPT nanofibers should be subjected to the Brunauer−Emmett−Teller (BET) measurement in order to provide the practical information about possible applications, the MPT nanofibers confined within porous alumina template are applied for BET measurement due to the difficulties in preparation of a large amount of sample (0.1−1 g) required for the measurement: A single template of the utilized porous alumina membrane (Whatman Anodisc 13) provides the pure MPT nanofibers of several tens of micrograms. Therefore, in this study, the estimated specific surface areas and pore volumes (per unit gram) do not indicate specific information on the MPT nanofibers itself due to the large weight contribution of the porous alumina. However, the BET parameters are provided for comparative studies to support the existence of the mesoporous phase within the porous alumina. Compared with the empty porous alumina that shows low BET surface area (S_{BET} = 9.4 m^2/g) and pore volume (V_p = 0.015 cm^3/g), the MPT nanofibers filled porous alumina membranes exhibit relatively high BET surface areas and pore volumes, although these composite membranes include a massive weight contribution (at least more than 90 wt %) by the porous alumina: S_{BET} = 23.7 m^2/g and V_p = 0.039 cm^3/g for MPT-1 and S_{BET} = 34.9 m^2/g and V_p = 0.058 cm^3/g for MPT-2. Moreover, unique adsorption−desorption hysteresis loops are observed from both samples, which is typically observed with mesoporous materials.[8] The adsorption branches of the MPT nanomaterials indicate that the major pore diameters are 4.2 and 5.6 nm for MPT-1 and MPT-2, respectively (insets of Figure 4). In addition, from the UV−Vis absorption spectra (Figure 5), the resulting MPT nanofibers exhibit characteristic absorption onsets near the bulk band gap (387 nm; 3.2 eV) of anatase titania,[9] regardless of the structural changes of wall thickness and pore size.

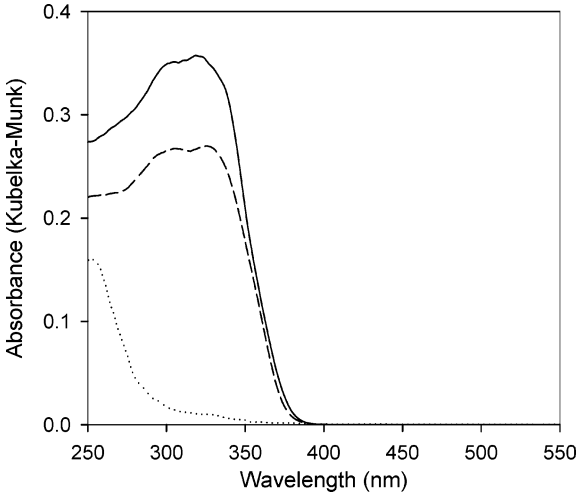

Figure 5. Absorption spectra of the mesoporous titania nanofibers of MPT-1 (solid line) and MPT-2 (dashed line) that are confined within porous alumina. The absorption spectrum for the empty porous alumina is also presented (dotted line). The absorption spectra are obtained by applying a Kubelka−Munk function to the diffuse reflectance spectra.

In summary, we have fabricated mesoporous titania nanofibers by using a bimodal templating concept, an amphiphilic triblock copolymer template within a porous alumina template. Resulting MPT nanofibers consist of nanocrystalline anatase titania, and the pore size can be easily controlled with the utilized amount of titania precursor. Due to unique characterestics of these MPT nanofibers, they can be hopefully applied to the fields of photocatalysis, energy conversion, and molecular sensing with size selectivity.

Acknowledgment. This work was financially supported by a National Research Laboratory (Grant No. M1-0302-00-0027) program and a National R & D Project for Nano-Science and Technology (Grant No. M1-0214-00-0021). We are thankful for the instrumental support from the equipment facility of CRM-KOSEF.

Supporting Information Available: Experimental and instrumental details (PDF). These materials are available free of charge via the Internet at http://pubs.acs.org.

CM050603F

(6) (a) Yang, P.; Deng, T.; Zhao, D.; Feng, P.; Pine, D.; Chmelka, B. F.; Whitesides, G. M.; Stucky, G. D. *Science* **1998**, *282*, 2244. (b) Chae, W.-S.; Lee, S.-W.; Im, S.-J.; Moon, S.-W.; Zin, W.-C.; Lee, J.-K.; Kim, Y.-R. *Chem. Commun*. **2004**, 2554.
(7) Klug, H. P.; Alexander, L. E. *X-ray Diffraction Properties for Polycrystalline and Amorphous Materials*; Wiley: New York, 1974.
(8) (a) Bagshaw, S. A.; Prouzet, E.; Pinnavaia, T. J. *Science* **1995**, *269*, 1242. (b) Blin, J. L.; Lesieur, P.; Stébé, M. J. *Langmuir* **2004**, *20*, 491. (c) Sayari, A.; Yang, Y. *Chem. Commun*. **2002**, 2582.
(9) (a) Linsebigler, A. L.; Lu, G.; Yates, Jr., J. T. *Chem. Rev*. **1995**, *95*, 735. (b) Kavan, L.; Grätzel, M.; Gilbert, S. E.; Klemenz, C.; Scheel, H. J. *J. Am. Chem. Soc*. **1996**, *118*, 6716.